

Cite this: *Nanoscale Adv.*, 2020, 2, 648Received 15th November 2019  
Accepted 8th January 2020

DOI: 10.1039/c9na00721k

rsc.li/nanoscale-advances

## Silver nanoparticles modulate lipopolysaccharide-triggered Toll-like receptor signaling in immune-competent human cell lines†

Anda R. Gliga,<sup>ab</sup> Jessica De Loma,<sup>id a</sup> Sebastiano Di Bucchianico,<sup>id a</sup>  
Sara Skoglund,<sup>id c</sup> Sandeep Keshavan,<sup>b</sup> Inger Odnevall Wallinder,<sup>id c</sup>  
Hanna L. Karlsson<sup>\*a</sup> and Bengt Fadeel<sup>id \*b</sup>

Silver (Ag) nanoparticles are commonly used in consumer products due to their antimicrobial properties. Here we studied the impact of Ag nanoparticles on immune responses by using cell lines of monocyte/macrophage and lung epithelial cell origin, respectively. Short-term experiments (24 h) showed that Ag nanoparticles reduced the lipopolysaccharide (LPS)-induced secretion of pro-inflammatory cytokines in THP-1 cells under serum-free conditions. ICP-MS analysis revealed that cellular uptake of Ag was higher under these conditions. Long-term exposure (up to 6 weeks) of BEAS-2B cells to Ag nanoparticles also suppressed pro-inflammatory cytokine production following a brief challenge with LPS. Experiments using reporter cells revealed that Ag nanoparticles as well as AgNO<sub>3</sub> inhibited LPS-triggered Toll-like receptor (TLR) signaling. Furthermore, RNA-sequencing of BEAS-2B cells indicated that Ag nanoparticles affected TLR signaling pathways. In conclusion, Ag nanoparticles reduced the secretion of pro-inflammatory cytokines in response to LPS, likely as a result of the release of silver ions leading to an interference with TLR signaling. This could have implications for the use of Ag nanoparticles as antibacterial agents. Further *in vivo* studies are warranted to study this.

Silver (Ag) nanoparticles are one of the most widely used nanomaterials in consumer products, and this has raised concerns regarding their potential adverse effects on human health.<sup>1</sup> It is debated whether or not Ag nanoparticles pose any *novel* risks that are fundamentally different from other forms of Ag including colloidal Ag.<sup>2–5</sup> However, there is ample evidence

that Ag nanoparticles exert cytotoxic effects towards human cells in addition to the well-known anti-bacterial effects, and some studies have suggested that this could be due, at least in part, to a Trojan horse mechanism whereby Ag nanoparticles are internalized by cells and subsequently undergo dissolution intracellularly with release of Ag ions.<sup>6–8</sup> Furthermore, particle size is also a key parameter, as demonstrated in several recent studies.<sup>7,9,10</sup> Indeed, we previously reported that 10 nm Ag nanoparticles were more cytotoxic and released more Ag when compared with larger Ag nanoparticles (75 nm) following incubation in cell culture medium.<sup>7</sup> Thus, the cytotoxicity of Ag nanoparticles is linked both to particle size and to ion release. However, ‘all that is silver is not toxic’, and recent studies have shown that aging of Ag ions in cell culture medium for 3 or more hours significantly attenuated toxicity towards a murine macrophage-like cell line.<sup>11</sup>

Since Ag nanoparticles are widely used for their antibacterial properties, it is important to determine whether these particles exert any immunosuppressive effects on immune-competent cells. To date, the findings with regards to the impact of Ag nanoparticles on cells of the innate immune system – the first line of cellular defense against microbial infection – are contradictory. Hence, Ag nanoparticles were reported to trigger the secretion of pro-inflammatory IL-1 $\beta$  in primary human monocytes as well as in the human THP-1 cell line, a commonly used model of monocytes.<sup>12,13</sup> Using microarray analysis, Lim *et al.* found that Ag nanoparticles induced upregulation of IL-8 (also known as CXCL8) in macrophage-like U937 cells, while pro-inflammatory cytokines such as IL-1 $\beta$ , IL-6, and TNF- $\alpha$  were not found to be significantly increased.<sup>14</sup> On the other hand, Ag nanoparticles were shown to suppress *Mycobacterium tuberculosis*-induced IL-1 $\beta$  production in primary human monocyte-derived macrophages.<sup>15</sup> In the latter study, the suppressive effects on IL-1 $\beta$  release were not reproduced with soluble Ag ions. The aim of the present study was to examine the impact of Ag nanoparticles on immune-competent cells exposed to bacterial lipopolysaccharide (LPS). To this end, we utilized citrate-coated Ag nanoparticles and studied their effects on

<sup>a</sup>Division of Biochemical Toxicology, Institute of Environmental Medicine, Karolinska Institutet, Stockholm, Sweden. E-mail: hanna.l.karlsson@ki.se

<sup>b</sup>Division of Molecular Toxicology, Institute of Environmental Medicine, Karolinska Institutet, Stockholm, Sweden. E-mail: bengt.fadeel@ki.se

<sup>c</sup>Department of Chemistry, Surface and Corrosion Science, KTH Royal Institute of Technology, Stockholm, Sweden

† Electronic supplementary information (ESI) available: Table S1: summary of particle characterization in BEGM; Table S2: canonical pathway analysis of RNA-seq data; Table S3: gene ontology enrichment analysis. See DOI: 10.1039/c9na00721k



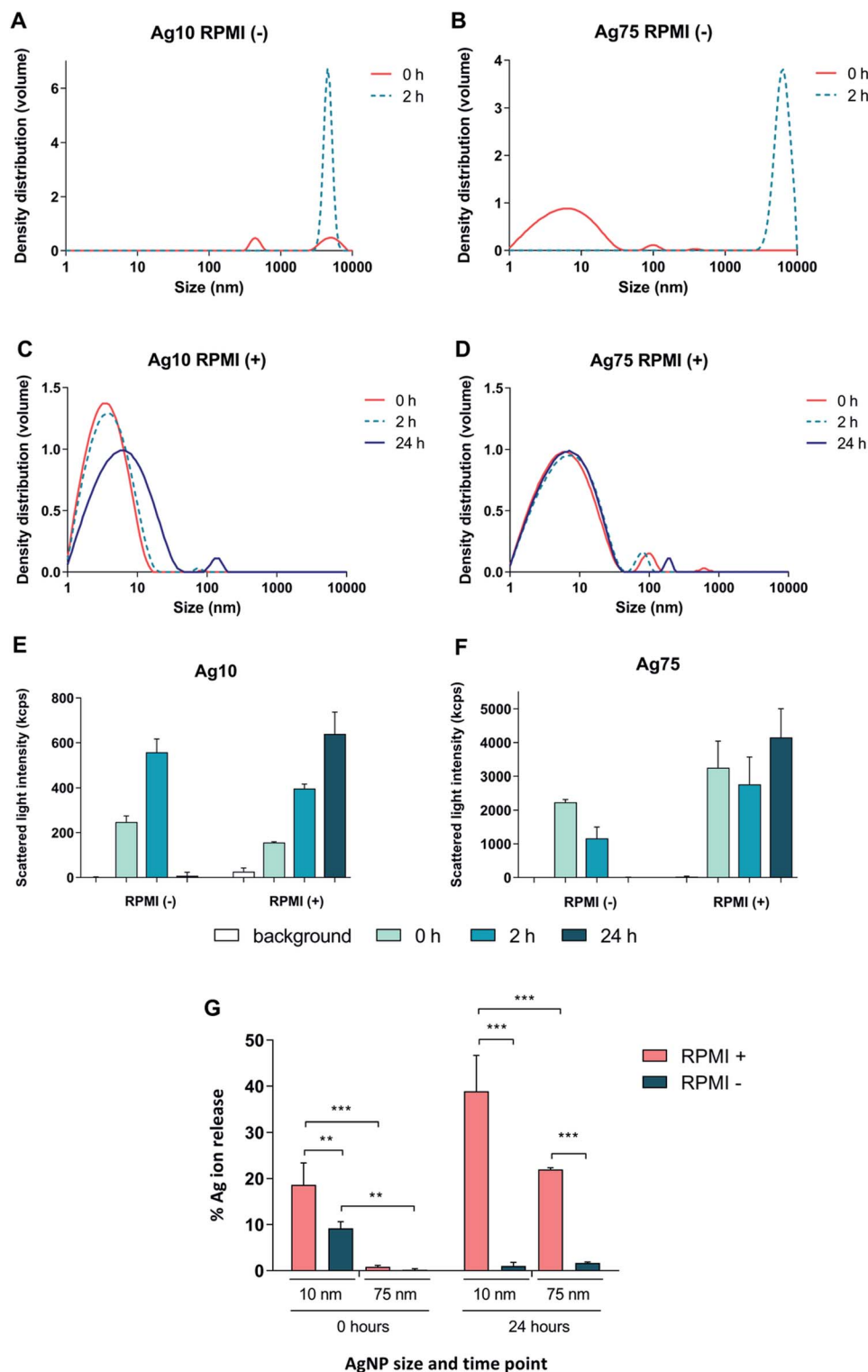


**Fig. 1** Characterization of Ag nanoparticles in RPMI-1640 cell medium. (A–F) The hydrodynamic size distribution of Ag nanoparticles ( $10 \mu\text{g mL}^{-1}$ ) was determined by PCCS and is expressed as density distribution by volume and was performed in RPMI-1640 medium without (A and B) or with 10% FBS (C and D). The variation in intensity of the scattered light over time for Ag10 (E) and Ag75 (F) is also shown. (G) The release of Ag in RPMI medium with or without 10% FBS after 0 h and 24 h for Ag10 and Ag75 ( $10 \mu\text{g mL}^{-1}$ ) was determined by ICP-MS. Results are expressed as the percentage of released silver compared to the total mass of silver (experimentally determined). Results are presented as mean values  $\pm$  S.D. ( $n = 3$ ). Significant results are marked with asterisks (\*  $p$ -value < 0.05, \*\*  $p$ -value < 0.01, \*\*\*  $p$ -value < 0.001).



cytokine secretion in macrophage-differentiated THP-1 cells and bronchial epithelial BEAS-2B cells, following short- or long-term exposure. In addition, we used a reporter cell line to elucidate whether Ag nanoparticles act directly on Toll-like receptors (TLRs), important pathogen recognition receptors expressed on lung epithelial cells, macrophages, and other immune cells.<sup>16</sup>

First, we tested whether Ag nanoparticles (10 nm and 75 nm) showed any immunosuppressive or anti-inflammatory effects in macrophage-differentiated THP-1 cells. THP-1 cells are commonly used as a model of innate immune cells and previous studies have shown that these cells are capable of producing a relevant repertoire of cytokines in response to LPS.<sup>17</sup> THP-1 cells can grow either in medium supplemented with fetal bovine serum (FBS) or in serum-free conditions. For comparison, BEAS-2B cells (see below) are cultured in serum-free medium supplemented with specific growth factors.<sup>18</sup> Since the presence of proteins can alter the characteristics and the ensuing biological behavior of nanoparticles,<sup>19</sup> we decided to investigate potential differences between the two cell culture conditions in terms of particle agglomeration/intensity of scattered light as well as release of Ag in cell culture medium. Particle agglomeration, sedimentation, and dissolution are processes that occur in parallel. Consequently, the intensity of the scattered light increases in a non-linear manner with increasing size and number of particles in the dispersion and decreases with particle sedimentation and dissolution.<sup>7,20</sup> Our results showed that the 10 nm particles and 75 nm particles displayed a more pronounced sedimentation in serum-free cell culture medium when compared to medium supplemented with 10% FBS (Fig. 1A–F). We also determined the release of Ag in different cell culture media by using inductively coupled plasma mass spectrometry (ICP-MS), and observed that the 10 nm particles released significantly more Ag when compared to the 75 nm particles, and this was more pronounced in cell culture medium supplemented with FBS (Fig. 1G). The increased release of Ag in the presence of serum proteins could be related to the high affinity of Ag for proteins that can shift the reaction equilibrium towards the solution. Overall, the Ag nanoparticles displayed reduced agglomeration and sedimentation and higher release of Ag in cell culture medium supplemented with 10% serum as compared to the serum-free conditions. We then evaluated the toxicity of the Ag nanoparticles in differentiated THP-1 cells using the Alamar Blue assay which reports the metabolic capacity of cells. Our results showed a dose-dependent toxicity in cells under serum-free conditions with cytotoxicity noted already at 5  $\mu\text{g mL}^{-1}$  (Fig. 2A and B). In addition, 10 nm particles were more cytotoxic than 75 nm particles. Furthermore, we found that the cellular content of Ag was, overall, higher in cells maintained in serum-free medium and higher for the 10 nm particles as compared to the 75 nm particles (at 5  $\mu\text{g mL}^{-1}$ ) (Fig. 2C). The higher cellular content of Ag under serum-free conditions could be explained by a greater particle sedimentation, leading to an increased contact between nanoparticles and cells. Indeed, higher uptake of citrate-capped Ag nanoparticles (75 nm) by THP-1 cells under serum-free culture conditions was reported in a previous

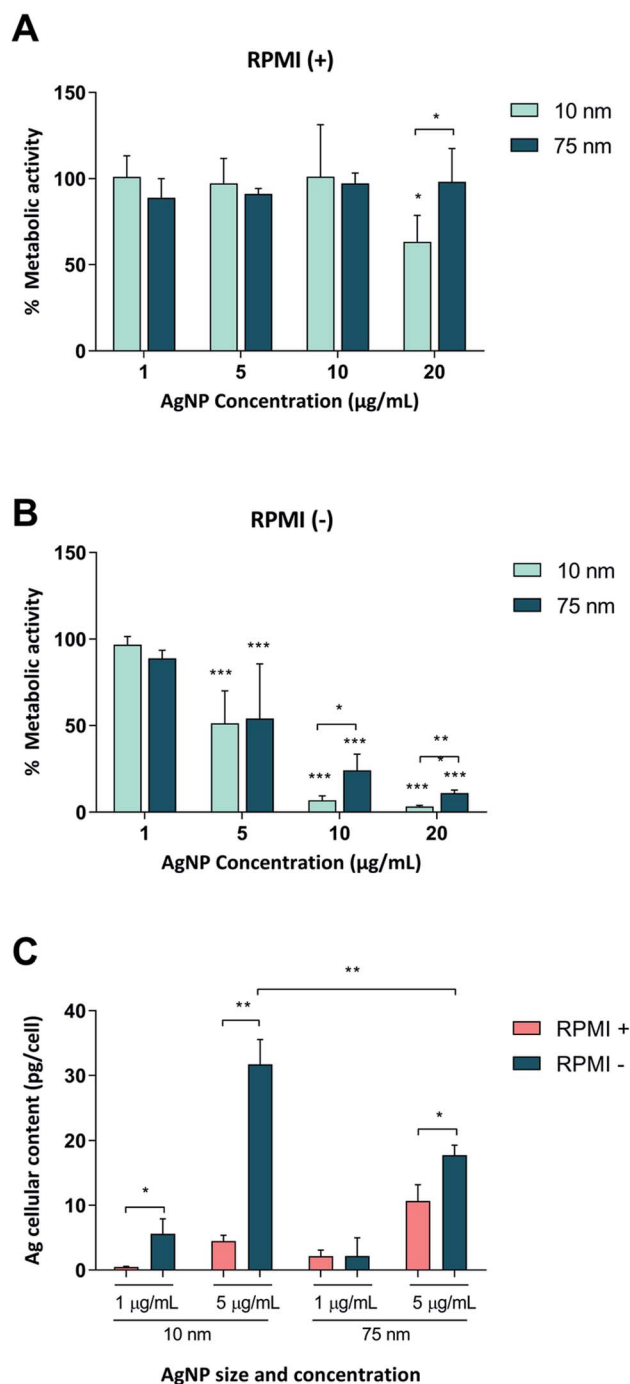


Fig. 2 Cytotoxicity of Ag nanoparticles in macrophage-like THP-1 cells. THP-1 cells were differentiated into macrophage-like cells followed by exposure for 24 h to 10 and 75 nm Ag nanoparticles in medium containing 10% FBS (A) or no serum (B). Cell viability was assessed by the Alamar Blue assay and expressed as % metabolic activity as compared to the untreated control. Results are presented as mean values  $\pm$  S.D. ( $n = 4$  for Ag10;  $n = 3$  for Ag75). Significant results are marked with asterisks (\*  $p$ -value < 0.05, \*\*  $p$ -value < 0.01, \*\*\*  $p$ -value < 0.001). (C) Cellular Ag content in human THP-1 cells differentiated into macrophage-like cells. Cells were exposed for 24 h to 1 or 5  $\mu\text{g mL}^{-1}$  of Ag nanoparticles in medium with or without 10% FBS. Ag content was determined by ICP-MS and expressed as pg per cell. Results are shown as mean values  $\pm$  S.D. ( $n = 3$ ). Significant results marked with asterisks (\* $p$  < 0.05, \*\* $p$  < 0.01, \*\*\* $p$  < 0.001).



study.<sup>21</sup> Notably, even though the Ag particles displayed a higher release of Ag in cell culture medium supplemented with FBS, as noted above, this did not translate into stronger toxicity, possibly due to the fact that the released Ag has a high affinity for serum proteins and therefore is less bioavailable. Hence, the results speak in favour of a Trojan horse-like mechanism whereby particle uptake is followed by intracellular dissolution.

Next, we exposed macrophage-like THP-1 cells to  $5 \mu\text{g mL}^{-1}$  Ag nanoparticles both in serum-free and serum-supplemented cell medium for 24 h followed by challenge with LPS, and then evaluated the secretion of pro-inflammatory cytokines. Our results showed that LPS triggered the secretion of IL-1 $\beta$ , IL-6, and TNF- $\alpha$ , but not IL-8/CXCL8 (Fig. 3A–D). In serum-containing medium, the 10 nm and 75 nm particles did not alter the LPS-triggered cytokine secretion, although a non-significant reduction of IL-6 secretion was noted in cells exposed to the 10 nm particles. However, in serum-free conditions the 10 nm particles, but not the 75 nm particles, significantly reduced the LPS-triggered secretion of pro-inflammatory IL-1 $\beta$ , TNF- $\alpha$ , and IL-6 (Fig. 3A–C). These results suggest that 10 nm Ag nanoparticles have immunosuppressive properties. Our findings are in agreement with a previous study showing that citrate-capped Ag nanoparticles (20 nm) suppressed *M. tuberculosis*-induced production of IL-1 $\beta$  in human monocyte-

derived macrophages.<sup>15</sup> It is also noteworthy that ultra-small Ag nanoparticles (<10 nm) were shown to attenuate airway inflammation and hyperresponsiveness in a mouse model of allergic airway disease.<sup>22</sup> The present results are, however, in contrast to other studies in which Ag nanoparticles were found to trigger *activation* of immune cells with secretion of pro-inflammatory cytokines.<sup>12,13</sup> The differences could be due to differences in particle properties or the use of different cell models, and may also be explained by different exposure regimens (*i.e.*, single *versus* repeated administration of Ag nanoparticles to cells).<sup>23</sup> Moreover, endotoxin contamination is a factor that cannot be ignored and may confound the data.<sup>24</sup>

We then asked whether similar effects on cytokine responses occurred following long-term exposure to Ag nanoparticles. To this end, we used the human bronchial epithelial cell line, BEAS-2B. The latter cells were suggested to exhibit high similarities in gene expression pattern to primary cells and are maintained under serum-free conditions which is more relevant for lung cells.<sup>20</sup> For characterization of the nanoparticles in relevant cell culture medium, see ESI Table S1.† We previously reported on the cytotoxicity of Ag nanoparticles towards BEAS-2B cells at weekly intervals of exposure up to 6 weeks using the Alamar Blue assay.<sup>18</sup> We also performed colony formation efficiency (CFE) assays in the latter study, and noted no effects

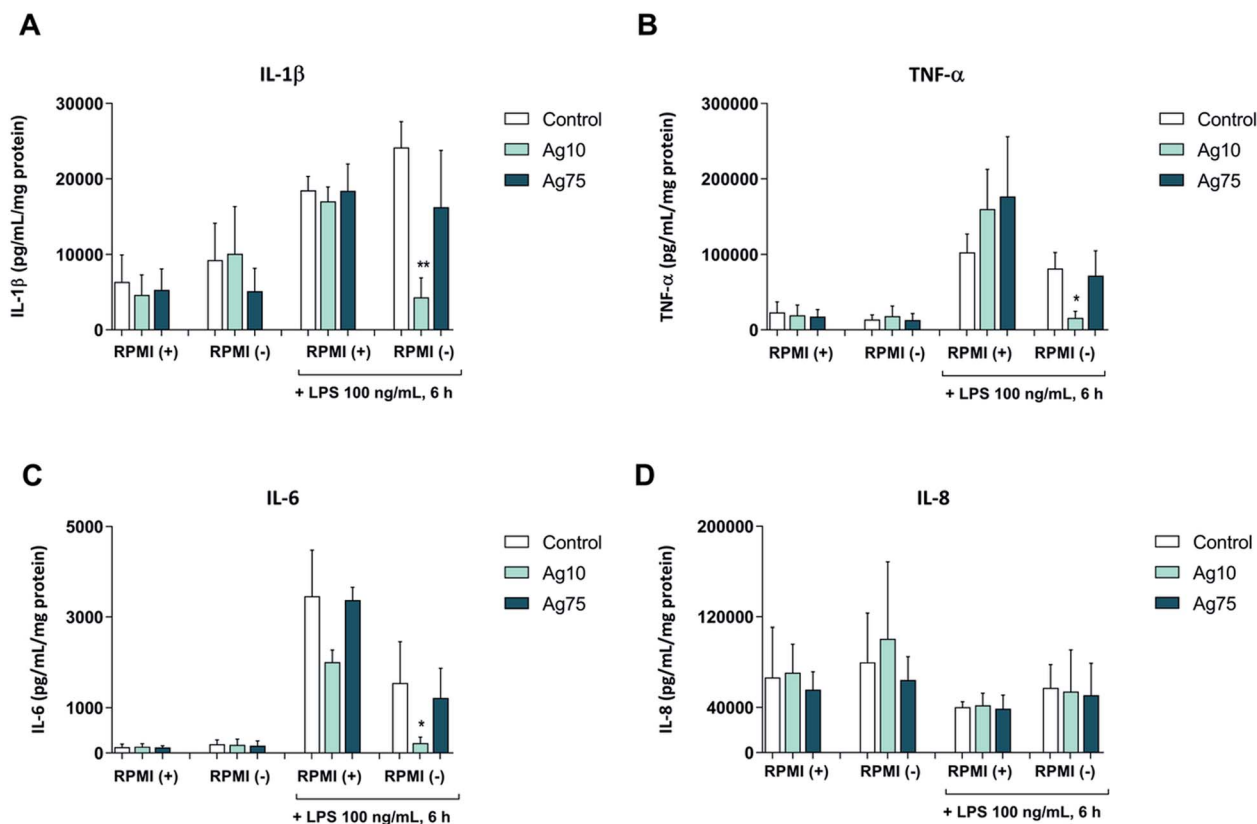


Fig. 3 Ag nanoparticles modulate macrophage responses to bacterial LPS in serum-free medium. Cytokine secretion following short-term (24 h) exposure to  $5 \mu\text{g mL}^{-1}$  Ag nanoparticles, as well as following LPS challenge, was determined using a multiplex assay. Cells were maintained in RPMI-1640 medium with (+) or without (-) 10% FBS. The following cytokines were analyzed: IL-1 $\beta$  (A), TNF- $\alpha$  (B), IL-6 (C), IL-8 (D). Cytokine concentrations were normalized to the protein content and expressed as pg/mL/mg protein. Results are presented as mean values  $\pm$  S.D. ( $n = 3$ ). Significant results are marked with asterisks (\*  $p$ -value < 0.05, \*\*  $p$ -value < 0.01).



at 3 weeks, while the 10 nm particles (but not the 75 nm particles) slightly reduced the CFE at week 6.

As shown in Fig. 4A, both basal and LPS-induced levels of IL-6 were suppressed in BEAS-2B cells exposed for 3 weeks to a low dose ( $1 \mu\text{g mL}^{-1}$ ) of Ag nanoparticles. Notably, following LPS challenge, the 10 nm particles displayed a stronger effect on IL-6 secretion when compared to the 75 nm particles. Furthermore, after 6 weeks, a similar pattern was observed for IL-6 (Fig. 4B). For IL-8/CXCL8, the LPS-induced secretion was reduced by the 10 nm particles, but not by the 75 nm particles after 3 weeks (Fig. 4C) as well as after 6 weeks (Fig. 4D), while there was no effect on the basal levels of IL-8/CXCL8. The basal levels of IL-1 $\beta$  were reduced by both Ag nanoparticles after 3 weeks whereas only the 10 nm particles reduced IL-1 $\beta$  formation in response to LPS (Fig. 4E). Similarly, after 6 weeks of exposure the IL-1 $\beta$  levels were lower for cells exposed to Ag nanoparticles when compared to control cells (Fig. 4F). Ag nanoparticles also reduced the levels of TNF- $\alpha$  following LPS exposure (Fig. 4G) and this was more pronounced for the 10 nm particles when compared to the 75 nm particles (at 3 weeks of exposure). After 6 weeks of exposure to Ag nanoparticles, LPS-induced TNF- $\alpha$  levels were low, and the impact of the Ag nanoparticles was not very evident (data not shown). The secretion of IL-1ra, an IL-1 receptor antagonist, was reduced in response to LPS exposure and its expression was suppressed by the 10 nm Ag particles, but not by the 75 nm particles (at 6 weeks of exposure) (Fig. 4H). No significant inhibition was noted for IL-10 or MIP-1 $\alpha$  (also known as CCL3) (data not shown). In conclusion, long-term exposure of human lung cells to Ag nanoparticles reduced the secretion of pro-inflammatory cytokines in response to a brief challenge with LPS, and these effects were more pronounced for the smaller Ag particles (10 nm).

Furthermore, to shed light on the underlying mechanism, we employed TLR reporter cells. TLR2 is a receptor that is activated by LPS in a response that depends on LPS-binding protein (LBP) and is enhanced by CD14.<sup>25</sup> The HEK-Blue™ hTLR2 cell line was generated by co-transfection of HEK293 cells with human TLR2 and CD14 along with the NF- $\kappa$ B/AP-1-secreted embryonic alkaline phosphatase (SEAP) reporter gene.<sup>26</sup> Once TLR2 signaling is initiated, NF- $\kappa$ B and AP-1 are activated, which leads to the secretion of SEAP which is detected in cell supernatants to quantify NF- $\kappa$ B activation. Our results showed that treatment with Ag nanoparticles alone did not impact on TLR2 activation (Fig. 5A). When challenged with LPS, there was an approx. 16-fold increase in reporter activation, and when the cells were co-treated with Ag nanoparticles and LPS there was a significant and dose-dependent reduction in reporter activation as compared to treatment with LPS alone. The inhibition was more potent for the 10 nm particles (Fig. 5A). These results provide evidence that the immunomodulatory effects of the Ag nanoparticles are mediated, at least in part, through the inhibition of TLR activation. In order to address whether the observed effect was related to Ag ions, reporter cells were also subjected to treatment with AgNO<sub>3</sub> with or without LPS. As shown in Fig. 5B, the Ag salt potently suppressed LPS-induced signaling. Finally, to further assess whether the effect was specific, reporter cells were exposed to TiO<sub>2</sub> NPs (primary particle size: 5 nm). The

latter NPs had no effect on LPS-triggered TLR signaling (Fig. 5C), thus supporting the view that the observed effects were specific for the Ag nanoparticles and likely due to the release of Ag ions.

Transcriptomics approaches are gaining traction in toxicological research and are regarded as a robust tool for identifying altered biological pathways, modes-of-action of toxicants, and biomarkers of toxicity.<sup>27</sup> Indeed, we and others have applied so-called next-generation sequencing to investigate mechanisms of nanoparticle-induced toxicity in cells and in intact organisms.<sup>28–30</sup> For instance, using RNA-seq, we could show that cerium oxide nanoparticles inhibited differentiation of neural stem cells.<sup>31</sup> In addition, we have applied RNA-seq to explore the effects of long-term exposure to Ag nanoparticles ( $1 \mu\text{g mL}^{-1}$ ) in BEAS-2B cells.<sup>18</sup> In the present study, we repurposed the previously obtained RNA-seq data and performed canonical pathway analysis by using the Ingenuity Pathway Analysis (IPA) software in order to explore gene expression changes related to immune function in cells exposed to Ag nanoparticles for 6 weeks. Pathways filtered for immune function are shown in ESI Table S2.† The genes corresponding to each pathway are also shown; the color coding indicates the direction of the gene expression change: red, upregulation, and blue, downregulation as compared to untreated cells. Hence, we noted that the gene encoding IL-1 $\alpha$ , a constitutively expressed pro-inflammatory cytokine, along with the genes encoding IL-1 $\beta$  and IL-18, inducible cytokines released upon inflammasome activation,<sup>32</sup> were all downregulated in BEAS-2B cells by Ag nanoparticles. Furthermore, *MYD88*, encoding an adaptor protein required for NF- $\kappa$ B activation downstream of TLRs was also downregulated.<sup>16</sup> We also performed gene ontology enrichment analysis and found that all of the top-hierarchical ontologies for the “biological process” categories were related to TLR signaling pathways, including the TRIF-dependent, TLR4, TLR9, TLR2, TLR10, TLR5, TLR1:TLR2, TLR6:TLR2, TLR3 and MyD88-dependent TLR pathways (ESI Table S3†). The corresponding up- and downregulated genes are also shown. Notably, we did not find that the Ag nanoparticles affected the genes encoding LPS receptors (*i.e.*, TLR2, TLR4, CD14). In sum, our analysis of the RNA-seq results supports the view that long-term exposure of BEAS-2B cells to Ag nanoparticles (10 nm) could yield immunosuppressive effects, possibly through a transcriptional effect on TLR signaling pathways.

Sarkar *et al.* proposed that Ag nanoparticles could interfere with TLR signaling pathways that culminate in NF- $\kappa$ B activation.<sup>15</sup> The authors speculated that the upregulation of Hsp72 by Ag nanoparticles could potentially block the expression of pro-inflammatory cytokines by inhibition of the cytoplasmic translocation of HMGB1 in *M. tuberculosis*-infected macrophages. Our results demonstrated that Ag nanoparticles interfere with TLR-mediated NF- $\kappa$ B activation which, in turn, may explain the transcriptional effects we identified by RNA-seq. In another recent study, Gonzalez-Carter *et al.* demonstrated internalization of Ag nanoparticles in microglia, resident macrophages of the brain.<sup>33</sup> The Ag nanoparticles showed anti-inflammatory effects with a reduction of LPS-stimulated TNF- $\alpha$  production, in line with the present results. The latter effects



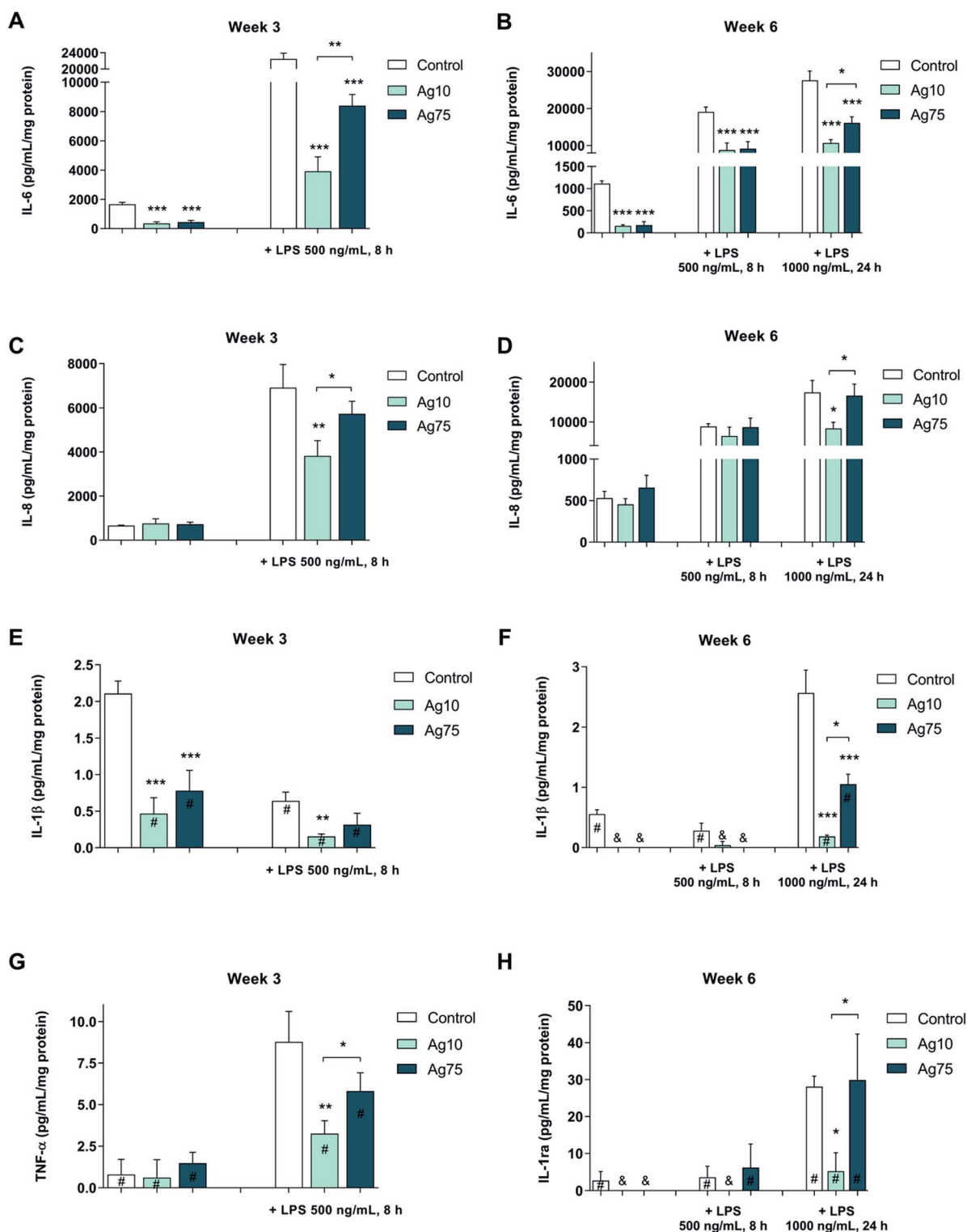


Fig. 4 Ag nanoparticles modulate LPS-triggered cytokines in human lung cells. Cytokine secretion following exposure for 3 or 6 weeks to Ag nanoparticles, with or without LPS challenge, was determined using the Bio-Plex® Pro multiplex assay. The following cytokines were evaluated: IL-6 at week 3 (A) and week 6 (B); IL-8 at week 3 (C) and week 6 (D); IL-1 $\beta$  at week 3 (E) and week 6 (F); TNF- $\alpha$  at week 3 (G), and IL-1ra at week 6 (H). Results for TNF- $\alpha$  at week 6 are not shown (no significant effects were noted). Cells were cultured in BEGM throughout the 3 to 6 week exposure and during LPS challenge. Cytokine levels were normalized to protein content and are expressed as pg/mL/mg protein. Results are presented as mean values  $\pm$  S.D. ( $n = 3$ ). Significant results are indicated with asterisks (\*  $p$ -value < 0.05, \*\*  $p$ -value < 0.01, \*\*\*  $p$ -value < 0.001). #, values outside the standard range; &, values below detection.



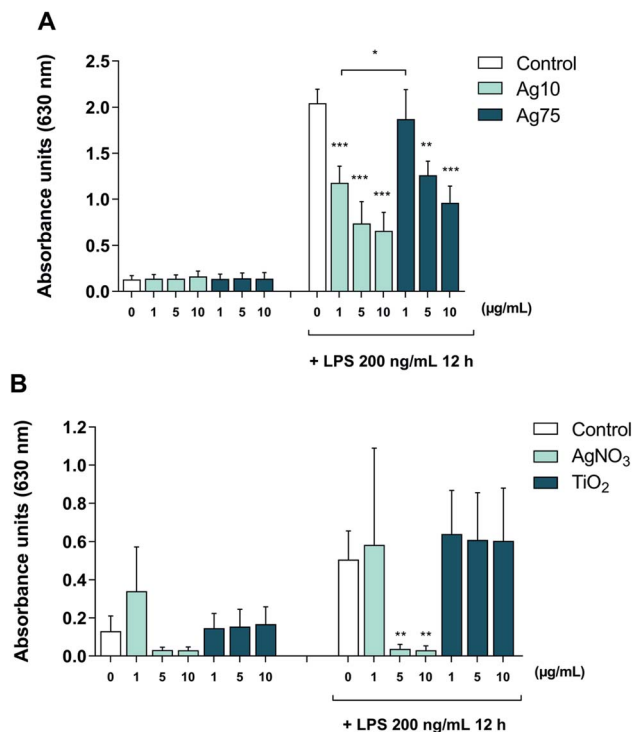


Fig. 5 Ag nanoparticles inhibit LPS-induced, TLR-mediated NF $\kappa$ B/AP-1 activation. The HEK-Blue™ hTLR2 reporter cell line co-transfected with CD14 was utilized to monitor LPS-induced TLR activation. Cells were monitored after exposure to the indicated concentrations of Ag nanoparticles (10 nm and 75 nm) with or without LPS challenge (100 ng mL<sup>-1</sup>) (A) or AgNO<sub>3</sub> with or without LPS challenge (100 ng mL<sup>-1</sup>) to address the role of Ag ions, or to TiO<sub>2</sub> nanoparticles with or without LPS challenge (100 ng mL<sup>-1</sup>) (B). Results shown are mean values  $\pm$  S.D. ( $n = 3$ ). Significant results are marked with asterisks (\*\*  $p$ -value < 0.01, \*\*\*  $p$ -value < 0.001).

were mirrored by AgNO<sub>3</sub>, though the effects were less pronounced. In contrast, other investigators have reported that Ag nanoparticles potentiated LPS-induced IL-8 and TNF- $\alpha$  production, but not LPS-induced IL-10 production.<sup>34</sup> Xu *et al.* found that PVP-coated Ag nanoparticles blocked the induction of oral tolerance to dietary antigen ovalbumin in mice.<sup>35</sup> It was noted that the released silver ions were the dominating factor. Hirai *et al.* reported that mice exposed to Ag nanoparticles and LPS developed allergic inflammation in response to silver.<sup>36</sup> The authors found that small NPs ( $\leq 10$  nm) transferred to lymph nodes and released ions more readily than large nanoparticles ( $> 10$  nm). Our results showed that the small (10 nm) particles released more Ag when compared to the larger (75 nm) particles, and we could show that this was more pronounced in cell culture medium supplemented with FBS, while the anti-inflammatory effects were evident under serum-free cell culture conditions. The latter observation can be explained by the increased cellular dose of Ag under these conditions. Taken together, it is likely that particle dissolution with intra- and/or extracellular release of ions accounts for the immunomodulatory effects of Ag nanoparticles. These effects may occur, at least in part, at the transcriptional level but could also transpire

through a direct inhibition of TLRs, as suggested by our experiments using reporter cells co-transfected with TLR2 and CD14. It is worth noting that other metals such as nickel (Ni<sup>2+</sup>) and cobalt (Co<sup>2+</sup>) were found to act directly on human (but not murine) TLR4.<sup>37,38</sup>

In conclusion, we explored the effects of Ag nanoparticles on the innate immune system by using different *in vitro* models. We could show that Ag nanoparticles elicited immunomodulatory effects following acute exposure of macrophage-like cells challenged with LPS. The latter effects were evidenced only in serum-free conditions, and as such, these effects cannot be explained by proteins present in the bio-corona.<sup>39</sup> We also found that long-term exposure of lung cells to Ag nanoparticles interfered with immune signaling by reducing basal levels of pro-inflammatory cytokines and altering cytokine secretion in response to LPS. These effects were shown to be related, at least in part, to interference with LPS-induced TLR signaling. Our studies also provided evidence that Ag ions are the likely mediators of these effects. Our results add to the growing body of literature suggesting that specific molecular interactions or interferences with intra- or extracellular proteins may underlie the toxicity of nanoparticles.<sup>40–42</sup> It has been pointed out that many applications of ‘nanosilver’ in consumer products appear unnecessary, exposing humans to possible health risks.<sup>43</sup> Indeed, the fact that Ag nanoparticles are able to suppress immune responses to LPS is relevant for the antibacterial uses of such nanoparticles, and may potentially counteract their beneficial effects, though further studies using relevant models of infection are required to appreciate the risk-benefit balance.

## Experimental section

### Nanoparticles

In the present study, 10 nm and 75 nm citrate-coated Ag-NPs (BioPure) were used. The latter are OECD reference materials. Both NPs were purchased from Nanocompositix (San Diego, CA) in the form of stock dispersions (1 mg mL<sup>-1</sup>) in aqueous 2 mM citrate. Dispersions in cell culture medium were prepared fresh prior to cell exposure. TiO<sub>2</sub> NPs (NM-101) were obtained from the nanomaterial repository at the Joint Research Centre (JRC) of the European Commission and were characterized and dispersed as previously described.<sup>17</sup>

### Nanoparticle characterization

Characterization of the nanoparticles in bronchial epithelial growth medium (BEGM) in terms of primary size (TEM), hydrodynamic size (photon cross-correlation spectroscopy, PCCS), Ag release (atomic absorption spectroscopy) was previously reported in Gliga *et al.*<sup>18</sup> The characterization of Ag nanoparticles in RPMI medium was performed in terms of (i) hydrodynamic size by photon cross-correlation spectroscopy (PCCS), and (ii) Ag release in cell medium by inductively coupled plasma mass spectrometry (ICP-MS). PCCS. Ag nanoparticles were dispersed in serum-free RPMI-1640 cell culture medium or in medium supplemented with 10% FBS at a concentration of 10  $\mu$ g mL<sup>-1</sup>. Samples were kept at 37 °C and



analyzed directly after dispersion (0 h) after 2 h and 24 h on a NanoPhox instrument (Sympatec, Germany). Data was analyzed and integrated using the Windox 5 software. Standard latex samples (Sympatec) and blank samples were analyzed prior to the measurements. Duplicate samples were measured three times each and data from each of the separate measurements was integrated to generate the final distributions. The intensity of the scattered light is presented as the mean of the six measurements with the corresponding standard deviation. **ICP-MS.** For evaluation of the release of Ag in cell culture medium, 10  $\mu\text{g mL}^{-1}$  Ag nanoparticle dispersions were prepared in RPMI-1640 medium, serum-free and supplemented with 10% FBS. The samples were handled right after preparation (0 h) or after 24 h (37 °C) by spinning down at 15 000 rpm for 1 h at 0 °C. Both the pellet (containing the particles) and the supernatant (containing the released Ag fraction) were collected for analysis. Mineralization of the samples was performed in 4% HCl and 40% HNO<sub>3</sub> for 48 h. Thereafter the samples were diluted to reach approx. 3.5% HNO<sub>3</sub> prior to the analysis. <sup>107</sup>Ag and <sup>109</sup>Ag isotopes were quantified using an iCAP Q instrument (ThermoScientific) running on KED mode. Calibration standards of 1, 5, 10, 50, 100, and 500 ppb Ag (Spectrascan) were prepared in 0.35% HCl and 3.5% HNO<sub>3</sub>. All samples were spiked with 5 ppb indium as an internal standard with a range of recovery between 85–105%. The limits of detection for the investigated isotopes were <0.05 ppb. Each sample was injected at least 5 times and the relative standard deviation (RSD) acceptance was set at 10%. The samples yielded acceptable recoveries of the Ag amount (99.29 ± 10.66) calculated as total theoretical Ag per total experimentally determined Ag. Results are expressed as % Ag released from the total Ag mass added, calculated using the formula:

$$\% \text{ released Ag} = \frac{2 \times \text{Ag in supernatant}}{\text{Ag in supernatant} + \text{Ag in pellet}} \times 100$$

### Endotoxin assessment

Endotoxin content was assessed using the chromogenic *Limulus* amoebocyte lysate (LAL) assay (Charles River Endosafe, Charleston, SC) according to the manufacturer's instructions. The endotoxin level was below 0.5 EU mL<sup>-1</sup> for 10 and 75 nm particles.

### Cell models

The human bronchial epithelial cell line BEAS-2B (ECCC) was cultured in bronchial epithelial cell growth medium (BEGM) (Lonza) supplemented with recombinant epidermal growth factor (EGF), hydrocortisone, insulin, bovine pituitary extract, GA-1000 (gentamicin sulfate and amphotericin-B), retinoic acid, transferrin, triiodothyronine and epinephrine (Lonza). Cells were cultured in vented flasks and plates pre-coated with: 0.01 mg mL<sup>-1</sup> fibronectin, 0.03 mg mL<sup>-1</sup> bovine collagen type I, 0.01 mg mL<sup>-1</sup> bovine serum albumin and 0.2% penicillin-streptomycin in BEGM additive free medium for 1–2 h prior to seeding. Cells were maintained in a humidified atmosphere at 37 °C, 5% CO<sub>2</sub>

and sub-cultured at 80% confluency. For the long-term exposure, cells were seeded in 6 well-plates (5 × 10<sup>3</sup> cells per cm<sup>2</sup>, 2 mL cell medium per well) and allowed to attach for approx. 2 h. Thereafter, cells were exposed to 1  $\mu\text{g mL}^{-1}$  Ag10 or Ag75 (approx. 0.2  $\mu\text{g cm}^{-2}$ ). Cells were split, counted, reseeded twice a week (5 × 10<sup>4</sup> cells per cm<sup>2</sup>, 2 mL cell medium per well) and re-exposed to Ag nanoparticles over 6 weeks. The human monocytic leukemia cell line THP-1 (ATCC) was cultured in RPMI-1640 medium (Sigma) supplemented with 2 mM L-glutamine, 100 U mL<sup>-1</sup> penicillin, 100  $\mu\text{g mL}^{-1}$  streptomycin, and 10% fetal bovine serum (FBS) in vented T-75 cm<sup>2</sup> flasks (Corning). Cells were maintained in a humidified incubator at 5% CO<sub>2</sub> and 37 °C. Cells were kept at a density of 2 × 10<sup>5</sup> and 1.5 × 10<sup>6</sup>. For differentiation into macrophage-like cells, THP-1 cells were seeded at a density of 10<sup>5</sup> cells per cm<sup>2</sup> in RPMI medium with 500 nM phorbol 12-myristate 13-acetate (PMA) (Sigma) for 24 h.

### RNA-seq and bioinformatics analysis

RNA sequencing and downstream analysis of the data was performed as previously described.<sup>18</sup> Briefly, following a 6 week exposure of BEAS-2B cells to 1  $\mu\text{g mL}^{-1}$  Ag nanoparticles (10 nm), RNA was extracted and RNA-seq was performed using an Illumina HiSeq2500 platform. The sequencing data are deposited at ArrayExpress, (accession number E-MTAB-6321). Differential gene expression was performed using the DESeq2 package and the downstream analysis (canonical pathway analysis) of the differentially expressed genes was performed using Ingenuity Pathway Analysis (IPA) software.<sup>44</sup> The canonical pathway analysis was repeated in the present study in order to obtain data using the most recent IPA content version (44691306, release date: 2018-06-14); data were filtered for pathways related to immune function, *e.g.*, cytokine signaling and cellular immune response categories. In addition, gene ontology enrichment analysis of the differentially expressed genes was performed using the online tool GOEast<sup>45</sup> using a Fischer exact test and Alexa's improved weighted scoring algorithm. The significance level of enrichment was set to a *p*-value of 0.05. The results are presented as the top-15 ontologies that correspond to the "biological process" domain, ordered according to their hierarchical level, *i.e.*, the ontologies that are the furthest down in the hierarchy have the highest level and thus are the most specific ones.

### Cell viability

THP-1 cells were differentiated into macrophage-like cells and exposed to 1–20  $\mu\text{g mL}^{-1}$  Ag nanoparticles both in complete medium and serum-free RPMI medium. Following exposure, cells were incubated with Alamar Blue 10% (Invitrogen), prepared in the corresponding media, for 1 h at 37 °C. Fluorescence was read on a microplate reader (Tecan Infinite F200) (excitation 560 nm; emission 590 nm). Experiments were repeated three times with technical triplicates per sample. Results are presented as % metabolic activity *versus* control.

### ICP-MS (cellular Ag content)

Macrophage-like THP-1 cells were exposed to 1 and 5  $\mu\text{g mL}^{-1}$  10 and 75 nm Ag nanoparticles in the presence or absence of





10% FBS for 24 h. At the end of the exposure, cells were harvested and counted. Samples were mineralized and analyzed as described above under 'nanoparticle characterization'. The limits of detection for the investigated isotopes were <0.05 ppb. Results are expressed as the mean amount of Ag in pg per cell.

### Cytokine analysis

Cytokine secretion after 3 and 6 weeks of Ag nanoparticle exposure in BEAS-2B cells and after 24 h exposure in THP-1 derived macrophages was determined by the Bio-Plex® Pro multiplex assay (Bio-Rad) using a selection of cytokines from the Human Cytokine Panel, Group I (week 3: IL-1 $\beta$ , IL-6, IL-8, TNF- $\alpha$ ; week 6: IL-1 $\beta$ , IL-1ra, IL-6, IL-8, IL-10, TNF- $\alpha$ , MIP-1 $\alpha$ ; 24 h: IL-1 $\beta$ , IL-6, IL-8, TNF- $\alpha$ ). In addition to the basal cytokine secretion, we also tested cytokine release following challenge with LPS (from *Escherichia coli* 0111:B4, Sigma-Aldrich) in THP-1 cells (100 ng mL<sup>-1</sup>, 6 h) and BEAS-2B cells (500 ng mL<sup>-1</sup>, 8 h and 1000 ng mL<sup>-1</sup>, 24 h). Following exposure, the supernatants were collected and stored at -80 °C for analysis. The multiplex analysis was performed according to the manufacturer's instructions and the data was acquired on a Bio-Plex® 200 system (Bio-Rad). The cytokine concentrations were normalized to the protein content and expressed as pg cytokine/mL/mg protein.

### TLR2-dependent NF $\kappa$ B/AP-1 activation

The HEK-Blue™ hTLR2 cell line (InvivoGen) was cultured in DMEM growth medium containing 4.5 g L<sup>-1</sup> glucose and supplemented with 10% FBS, 50 U mL<sup>-1</sup> penicillin, 50 mg mL<sup>-1</sup> streptomycin, 100 mg mL<sup>-1</sup> Normocin™, 2 mM L-glutamine and 1  $\times$  HEK-Blue™ selection antibiotics mixture, according to the manufacturers' instruction. Cells were harvested and seeded in 96-well plates (50,000 cells per well). Cells were then exposed to Ag nanoparticles (10 nm and 75 nm), AgNO<sub>3</sub>, or TiO<sub>2</sub> nanoparticles (5 nm) at the indicated concentrations for 6 h followed by a 12 h challenge with LPS (100 ng mL<sup>-1</sup>) or medium alone. Exposures were performed in serum-free HEK-Blue™ detection medium (InvivoGen). TLR2-dependent, NF $\kappa$ B/AP-1-mediated SEAP (secreted embryonic alkaline phosphatase) production was quantified at 630 nm in a microplate reader (Tecan Infinite F200).

### Author contributions

A. R. G. performed *in vitro* experiments, bioinformatics analyses, and wrote the first draft of the manuscript; J. D. L. performed *in vitro* experiments and ICP-MS; S. B. and S. K. contributed to the *in vitro* experiments; S. S performed PCCS analysis supervised by I.O.W.; B. F. supervised the work and contributed to data analysis; H. L. K. initiated and supervised the study and contributed to data analysis; B. F. and H. L. K. wrote the manuscript and all authors approved the final version.

### Conflicts of interest

The authors have no conflicts of interest to declare.

### Acknowledgements

This work was supported by the Swedish Research Council for Health, Working Life and Welfare (FORTE, 2011-0832), the Swedish Research Council (VR, 2014-4598), and the European Commission through the Horizon2020 project BIORIMA (grant agreement no. 760928).

### References

- 1 S. W. P. Wijnhoven, W. J. G. M. Peijnenburg, C. A. Herberths, W. I. Hagens, A. G. Oomen, E. H. W. Heugens, B. Roszek, J. Bisschops, I. Gosens, D. Van De Meent, S. Dekkers, W. H. De Jong, M. van Zijverden, A. J. A. M. Sips and R. E. Geertsma, Nano-silver – a review of available data and knowledge gaps in human and environmental risk assessment, *Nanotoxicology*, 2009, 3(2), 109–138.
- 2 B. Nowack, H. F. Krug and M. Height, 120 years of nanosilver history: implications for policy makers, *Environ. Sci. Technol.*, 2011, 45(4), 1177–1183.
- 3 B. Schäfer, J. Tentschert and A. Luch, Nanosilver in consumer products and human health: more information required!, *Environ. Sci. Technol.*, 2011, 45(17), 7589–7590.
- 4 J. Costanza, A. M. El Badawy and T. M. Tolaymat, Comment on "120 years of nanosilver history: implications for policy makers", *Environ. Sci. Technol.*, 2011, 45(17), 7591–7592.
- 5 B. Nowack, H. F. Krug and M. Height, Reply to comments on "120 years of nanosilver history: implications for policy makers", *Environ. Sci. Technol.*, 2011, 45(17), 7593–7595.
- 6 E. J. Park, J. Yi, Y. Kim, K. Choi and K. Park, Silver nanoparticles induce cytotoxicity by a Trojan-horse type mechanism, *Toxicol. In Vitro*, 2010, 24(3), 872–878.
- 7 A. R. Gliga, S. Skoglund, I. O. Wallinder, B. Fadeel and H. L. Karlsson, Size-dependent cytotoxicity of silver nanoparticles in human lung cells: the role of cellular uptake, agglomeration and Ag release, *Part. Fibre Toxicol.*, 2014, 11, 11.
- 8 I. L. Hsiao, Y. K. Hsieh, C. F. Wang, I. C. Chen and Y. J. Huang, Trojan-horse mechanism in the cellular uptake of silver nanoparticles verified by direct intra- and extracellular silver speciation analysis, *Environ. Sci. Technol.*, 2015, 49(6), 3813–3821.
- 9 M. V. Park, A. M. Neigh, J. P. Vermeulen, L. J. de la Fonteyne, H. W. Verharen, J. J. Briedé, H. van Loveren and W. H. de Jong, The effect of particle size on the cytotoxicity, inflammation, developmental toxicity and genotoxicity of silver nanoparticles, *Biomaterials*, 2011, 32(36), 9810–9817.
- 10 R. F. Hamilton, S. Buckingham and A. Holian, The effect of size on Ag nanosphere toxicity in macrophage cell models and lung epithelial cell lines is dependent on particle dissolution, *Int. J. Mol. Sci.*, 2014, 15(4), 6815–6830.
- 11 J. N. Smith, D. G. Thomas, H. Jolley, V. K. Kodali, M. H. Littke, P. Munusamy, D. R. Baer, M. J. Gaffrey, B. D. Thrall and J. G. Teeguarden, All that is silver is not toxic: silver ion and particle kinetics reveals the role of silver ion aging and dosimetry on the toxicity of silver nanoparticles, *Part. Fibre Toxicol.*, 2018, 15(1), 47.



- 12 E. J. Yang, S. Kim, J. S. Kim and I. H. Choi, Inflammasome formation and IL-1 $\beta$  release by human blood monocytes in response to silver nanoparticles, *Biomaterials*, 2012, **33**(28), 6858–6867.
- 13 A. Murphy, A. Casey, G. Byrne, G. Chambers and O. Howe, Silver nanoparticles induce pro-inflammatory gene expression and inflammasome activation in human monocytes, *J. Appl. Toxicol.*, 2016, **36**(10), 1311–1320.
- 14 D. H. Lim, J. Jang, S. Kim, T. Kang, K. Lee and I. H. Choi, The effects of sub-lethal concentrations of silver nanoparticles on inflammatory and stress genes in human macrophages using cDNA microarray analysis, *Biomaterials*, 2012, **33**(18), 4690–4699.
- 15 S. Sarkar, B. F. Leo, C. Carranza, S. Chen, C. Rivas-Santiago, A. E. Porter, M. P. Ryan, A. Gow, K. F. Chung, T. D. Tetley, J. J. Zhang, P. G. Georgopoulos, P. A. Ohman-Strickland and S. Schwander, Modulation of human macrophage responses to *Mycobacterium tuberculosis* by silver nanoparticles of different size and surface modification, *PLoS One*, 2015, **10**(11), e0143077.
- 16 N. J. Gay, M. F. Symmons, M. Gangloff and C. E. Bryant, Assembly and localization of Toll-like receptor signalling complexes, *Nat. Rev. Immunol.*, 2014, **14**(8), 546–558.
- 17 K. Bhattacharya, G. Kiliç, P. M. Costa and B. Fadeel, Cytotoxicity screening and cytokine profiling of nineteen nanomaterials enables hazard ranking and grouping based on inflammogenic potential, *Nanotoxicology*, 2017, **11**(6), 809–826.
- 18 A. R. Gliga, S. Di Bucchianico, J. Lindvall, B. Fadeel and H. L. Karlsson, RNA-sequencing reveals long-term effects of silver nanoparticles on human lung cells, *Sci. Rep.*, 2018, **8**(1), 6668.
- 19 B. Fadeel, N. Feliu, C. Vogt, A. M. Abdelmonem and W. J. Parak, Bridge over troubled waters: understanding the synthetic and biological identities of engineered nanomaterials, *Wiley Interdiscip. Rev.: Nanomed. Nanobiotechnol.*, 2013, **5**(2), 111–129.
- 20 S. Di Bucchianico, A. R. Gliga, E. Åkerlund, S. Skoglund, I. O. Wallinder, B. Fadeel and H. L. Karlsson, Calcium-dependent cyto- and genotoxicity of nickel metal and nickel oxide nanoparticles in human lung cells, *Part. Fibre Toxicol.*, 2018, **15**(1), 32.
- 21 P. Krystek, K. Kettler, B. van der Wagt and W. H. de Jong, Exploring influences on the cellular uptake of medium-sized silver nanoparticles into THP-1 cells, *Microchem. J.*, 2015, **120**, 45–50.
- 22 H. S. Park, K. H. Kim, S. Jang, J. W. Park, H. R. Cha, J. E. Lee, J. O. Kim, S. Y. Kim, C. S. Lee, J. P. Kim and S. S. Jung, Attenuation of allergic airway inflammation and hyperresponsiveness in a murine model of asthma by silver nanoparticles, *Int. J. Nanomed.*, 2010, **5**, 505–515.
- 23 C. Aude-Garcia, F. Villiers, V. Collin-Faure, K. Pernet-Gallay, P. H. Jouneau, S. Sorieul, G. Mure, A. Gerdil, N. Herlin-Boime, M. Carrière and T. Rabilloud, Different in vitro exposure regimens of murine primary macrophages to silver nanoparticles induce different fates of nanoparticles and different toxicological and functional consequences, *Nanotoxicology*, 2016, **10**(5), 586–596.
- 24 Y. Li, Z. Shi, I. Radauer-Preiml, A. Andosch, E. Casals, U. Luetz-Meindl, M. Cobaleda, Z. Lin, M. Jaberi-Douraki, P. Italiani, J. Horejs-Hoeck, M. Himly, N. A. Monteiro-Riviere, A. Duschl, V. F. Puentes and D. Boraschi, Bacterial endotoxin (lipopolysaccharide) binds to the surface of gold nanoparticles, interferes with biocorona formation and induces human monocyte inflammatory activation, *Nanotoxicology*, 2017, **11**(9–10), 1157–1175.
- 25 R. B. Yang, M. R. Mark, A. Gray, A. Huang, M. H. Xie, M. Zhang, A. Goddard, W. I. Wood, A. L. Gurney and P. J. Godowski, Toll-like receptor-2 mediates lipopolysaccharide-induced cellular signalling, *Nature*, 1998, **395**(6699), 284–288.
- 26 S. P. Mukherjee, O. Bondarenko, P. Kohonen, F. T. Andón, T. Brzicová, I. Gessner, S. Mathur, M. Bottini, P. Calligari, L. Stella, E. Kisin, A. Shvedova, R. Autio, H. Salminen-Mankonen, R. Lahesmaa and B. Fadeel, Macrophage sensing of single-walled carbon nanotubes via Toll-like receptors, *Sci. Rep.*, 2018, **8**(1), 1115.
- 27 P. M. Costa and B. Fadeel, Emerging systems biology approaches in nanotoxicology: towards a mechanism-based understanding of nanomaterial hazard and risk, *Toxicol. Appl. Pharmacol.*, 2016, **299**, 101–111.
- 28 D. F. Simon, R. F. Domingos, C. Hauser, C. M. Hutchins, W. Zerges and K. J. Wilkinson, Transcriptome sequencing (RNA-seq) analysis of the effects of metal nanoparticle exposure on the transcriptome of *Chlamydomonas reinhardtii*, *Appl. Environ. Microbiol.*, 2013, **79**(16), 4774–4785.
- 29 N. Feliu, P. Kohonen, J. Ji, Y. Zhang, H. L. Karlsson, L. Palmberg, A. Nyström and B. Fadeel, Next-generation sequencing reveals low-dose effects of cationic dendrimers in primary human bronchial epithelial cells, *ACS Nano*, 2015, **9**(1), 146–163.
- 30 M. Zheng, J. Lu and D. Zhao, Toxicity and transcriptome sequencing (RNA-seq) analyses of adult zebrafish in response to exposure carboxymethyl cellulose stabilized iron sulfide nanoparticles, *Sci. Rep.*, 2018, **8**(1), 8083.
- 31 A. R. Gliga, K. Edoff, F. Caputo, T. Källman, H. Blom, H. L. Karlsson, L. Ghibelli, E. Traversa, S. Ceccatelli and B. Fadeel, Cerium oxide nanoparticles inhibit differentiation of neural stem cells, *Sci. Rep.*, 2017, **7**(1), 9284.
- 32 P. Broz and V. M. Dixit, Inflammasomes: mechanism of assembly, regulation and signalling, *Nat. Rev. Immunol.*, 2016, **16**(7), 407–420.
- 33 D. A. Gonzalez-Carter, B. F. Leo, P. Ruenraroengsak, S. Chen, A. E. Goode, I. G. Theodorou, K. F. Chung, R. Carzaniga, M. S. Shaffer, D. T. Dexter, M. P. Ryan and A. E. Porter, Silver nanoparticles reduce brain inflammation and related neurotoxicity through induction of H<sub>2</sub>S-synthesizing enzymes, *Sci. Rep.*, 2017, **7**, 42871.
- 34 V. Galbiati, L. Cornaghi, E. Gianazza, M. A. Potenza, E. Donetti, M. Marinovich and E. Corsini, In vitro



- assessment of silver nanoparticles immunotoxicity, *Food Chem. Toxicol.*, 2018, **112**, 363–374.
- 35 Y. Xu, H. Tang, H. Wang and Y. Liu, Blockade of oral tolerance to ovalbumin in mice by silver nanoparticles, *Nanomedicine*, 2015, **10**(3), 419–431.
- 36 T. Hirai, Y. Yoshioka, N. Izumi, K. Ichihashi, T. Handa, N. Nishijima, E. Uemura, K. Sagami, H. Takahashi, M. Yamaguchi, K. Nagano, Y. Mukai, H. Kamada, S. Tsunoda, K. J. Ishii, K. Higashisaka and Y. Tsutsumi, Metal nanoparticles in the presence of lipopolysaccharides trigger the onset of metal allergy in mice, *Nat. Nanotechnol.*, 2016, **11**(9), 808–816.
- 37 M. Schmidt, B. Raghavan, V. Müller, T. Vogl, G. Fejer, S. Tchaptchet, S. Keck, C. Kalis, P. J. Nielsen, C. Galanos, J. Roth, A. Skerra, S. F. Martin, M. A. Freudenberg and M. Goebeler, Crucial role for human Toll-like receptor 4 in the development of contact allergy to nickel, *Nat. Immunol.*, 2010, **11**(9), 814–819.
- 38 B. Raghavan, S. F. Martin, P. R. Esser, M. Goebeler and M. Schmidt, Metal allergens nickel and cobalt facilitate TLR4 homodimerization independently of MD2, *EMBO Rep.*, 2012, **13**(12), 1109–1115.
- 39 S. Juling, A. Niedzwiecka, L. Böhmert, D. Lichtenstein, S. Selve, A. Braeuning, A. F. Thünemann, E. Krause and A. Lampen, Protein corona analysis of silver nanoparticles links to their cellular effects, *J. Proteome Res.*, 2017, **16**(11), 4020–4034.
- 40 K. K. Comfort, E. I. Maurer, L. K. Braydich-Stolle and S. M. Hussain, Interference of silver, gold, and iron oxide nanoparticles on epidermal growth factor signal transduction in epithelial cells, *ACS Nano*, 2011, **5**(12), 10000–10008.
- 41 Z. Wang, S. Liu, J. Ma, G. Qu, X. Wang, S. Yu, J. He, J. Liu, T. Xia and G. B. Jiang, Silver nanoparticles induced RNA polymerase-silver binding and RNA transcription inhibition in erythroid progenitor cells, *ACS Nano*, 2013, **7**(5), 4171–4186.
- 42 Y. Miao, J. Xu, Y. Shen, L. Chen, Y. Bian, Y. Hu, W. Zhou, F. Zheng, N. Man, Y. Shen, Y. Zhang, M. Wang and L. Wen, Nanoparticle as signaling protein mimic: robust structural and functional modulation of CaMKII upon specific binding to fullerene C60 nanocrystals, *ACS Nano*, 2014, **8**(6), 6131–6144.
- 43 J. K. Schluesener and H. J. Schluesener, Nanosilver: application and novel aspects of toxicology, *Arch. Toxicol.*, 2013, **87**(4), 569–576.
- 44 A. Krämer, J. Green, J. Pollard Jr and S. Tugendreich, Causal analysis approaches in Ingenuity Pathway Analysis, *Bioinformatics*, 2014, **30**(4), 523–530.
- 45 Q. Zheng and X. J. Wang, GOEAST: a web-based software toolkit for gene ontology enrichment analysis, *Nucleic Acids Res.*, 2008, **36**, W358–W363.

